Supporting Information file

Heteroatom-Tuned σ–π Orbital Reorganization Enables Efficient Oxygen Reduction and Evolution Electrocatalysis Beyond Noble-Metal Catalysts

*K.M. Mithra [a], Prakash Govindaraj [b], S. Susanna Victoria Backiyaleela [a], Hern Kim [b], S. Sinthika [a, *], Rajkamal Anand [c, *]*

[a] Department of Physics and Research Centre, Lady Doak College, Affiliated to Madurai Kamaraj University, Madurai-625002, Tamil Nadu, India
[b] Department of Energy Science and Technology, Environmental Waste Recycle Institute, Myongji University, Yongin, Gyeonggi-do, 17058, Republic of Korea
[c] Institute of Advanced Aerospace Technology, Seoul National University, Gwanak-gu Gwanak-ro 1, Seoul 08826, Republic of Korea

**Corresponding authors: sinthika@ldc.edu.in (S Sinthika), rajkamalloyola@gmail.com (Rajkamal A)*

1. Computational Details

The adsorption energy of each adsorbate is defined by [1,2]

$$\Delta G = \Delta E + \Delta E_{ZPE} - T\Delta S + \Delta G_U + \Delta G_{pH} \quad (1)$$

where ΔE is the energy change from the DFT calculations, ΔE_{ZPE} is the zero-point energy, S is entropy, and T signifies the room temperature (298.15 K). The term ΔG_U = -eU, where U is the electrode potential and $\Delta G_{pH} = k_B T ln10 \times$ pH, pH value set to 0.

The ORR/OER process follows a four-electron transfer mechanism described by the following elementary reaction steps:

$$* + O_2(g) + H^+ + e^- \rightarrow OOH* \quad (\Delta G_1)$$

$$OOH* + H^+ + e^- \rightarrow O* + H_2O(l) \quad (\Delta G_2)$$

$$O* + H^+ + e^- \rightarrow OH* \quad (\Delta G_3)$$

$$OH* + H^+ + e^- \rightarrow * + H_2O(l) \quad (\Delta G_4)$$

Here, * represents the active metal center, and OOH*, O*, OH* are the intermediates formed during the reaction. The OER process is considered as the reverse of ORR steps. Among the reaction steps, the step that requires the highest Gibbs free energy change is considered as the rate determining step (RDS). The computational standard hydrogen electrode model presented by Nørskov et al. is used to evaluate the performance of the catalyst by finding the theoretical overpotential(η) using the formulae [3]

$$\eta_{ORR} = 1.23 - min(\Delta G_{1-4}) \quad (2)$$

$$\eta_{OER} = \max(\Delta G_{1-4}) - 1.23 \quad (3)$$

The formation energy (E_F) [4] and dissolution potential (U_{diss}) [5] was calculated using,

$$E_F = E_{TM@sub} - E_{TM} - E_{sub,} \quad (4)$$

$$U_{diss} = U^{\circ}_{diss(metal,bulk)} - E_F/eN \quad (5)$$

where $E_{TM@sub}$ and E_{sub} are the total energies of the system with the transition metal and the system without transition metal atom respectively, E_{TM} is the average energy of each transition

metal atom in its most stable bulk state, $U^{\circ}_{diss(metal,bulk)}$ and N represents the dissolution potential of the transition metal in its bulk state and number of electrons transferred during the process of dissolution respectively.

The energetically favored position of the B/P dopants in the SCS is identified by relative total energy calculation (ΔE_{rel}) given by,[6]

$$\Delta E_{rel} = E_{i}^{DFT} - E_{ref}^{DFT} \quad (6)$$

Where E_{i}^{DFT} and E_{ref}^{DFT} are the total energies of the system of interest and the reference system with highest positive value respectively. The site with the lowest (most negative) relative energy corresponds to the most thermodynamically stable configuration compared to the other sites.

Charge density difference (CDD) are calculated using,

$$\Delta\rho = \rho_{TM_{EN_4G}} - \rho_{TM} - \rho_{EN_4G} \quad (7)$$

where $\rho_{TM_{EN_4G}}$ and ρ_{EN_4G} represents the charge densities of the graphene nanoribbon substrate with and without the metal, respectively. ρ_{TM} is the charge density of the isolated TM in the same geometrical structure.

2. ML workflow: input features, models and metrics

For machine learning (ML) study, the ML datasets that encompass (i) the atomic, (ii) electronic, and (iii) environmental parameters — both intrinsic and DFT calculated parameters pertaining to the transition metal and the neighbouring dopant atoms were prepared. The atomic features were obtained from standard data and previous literature.[7,8] A total of 27 input features were considered. To avoid the heterogeneity introduced by asymmetric spin-resolved DOS that might pollute the feature representation in ML, we have uniformly employed the d band centres obtained from spin polarized calculations with total magnetic moment set as zero for all systems. For model training, we explored six different ML regression algorithms: random forest regression (RFR), gradient boosting regression (GBR), support vector regression (SVR), eXtreme Gradient Boosting (XGBoost), multiple linear regression (MLR), and Least Absolute Shrinkage and Selection Operator (LASSO). The dataset was randomly divided into training and test sets in an 80:20 ratio. The efficiency of an ML model was decided using the R^2 score

and the root mean squared error (RMSE). A higher R^2 and a lower RMSE value indicate the best model.

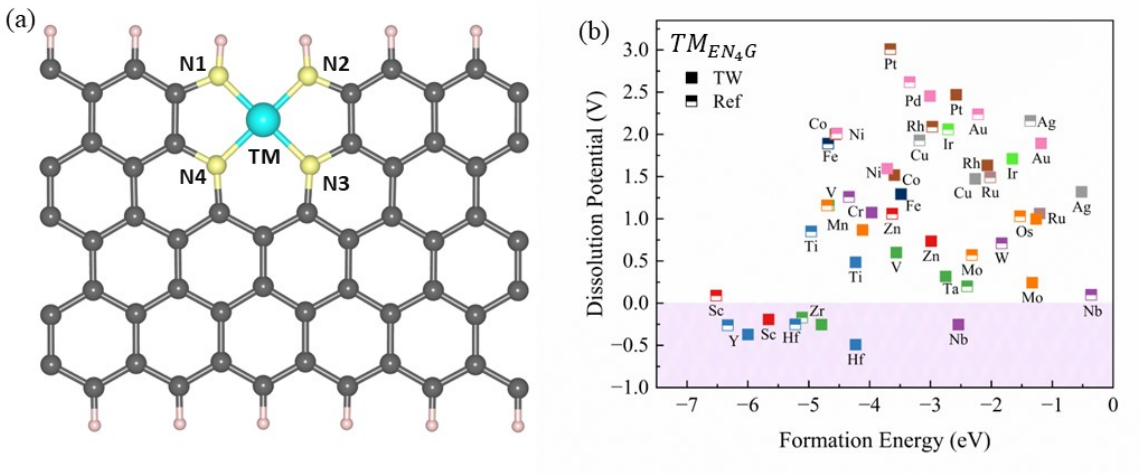

Figure S1. *a) Schematics and b) Graphical Plot of U_{diss} Vs E_F of* $^{TM_{EN_4Gs}}$

Table S1. *The average energies of each TM atom in the most stable bulk structure (E_{TM}) and the formation energies E_f, (eV) of TM atoms at each* $^{pristine-TM_{EN_4G}}$ *substrate.*

TM in EN_4-C	E_{TM} (eV/atom)	E_f (eV)		U_{diss} (V)	
		TW	Ref.	TW	Ref.
Sc	-6.48796	-5.66	-6.52	-0.19	0.09
Ti	-8.23464	-4.23	-4.96	0.49	0.85
V	-9.48292	-3.56	-4.67	0.60	1.16
Cr	-9.50967	-3.97	-4.34	1.07	1.26
Mn	-9.15592	-4.12	-4.70	0.87	1.16
Fe	-8.55038	-3.48	-4.68	1.29	1.89
Co	-7.36406	-3.60	-4.56	1.52	2.00
Cu	-4.237	-2.27	-3.18	1.47	1.93
Ni	-5.87033	-3.71	-4.54	1.60	2.01
Zn	-1.4628	-2.99	-3.63	0.73	1.06
Y	-6.43434	-6.00	-6.33	-0.37	-0.26
Zr	-8.51098	-4.79	-5.11	-0.25	0.17
Nb	-10.7775	-2.54	-0.36	-0.25	0.1
Mo	-11.4885	-1.33	-2.32	0.24	0.57

Ru	-9.80818	-1.21	-2.02	1.06	1.49
Rh	-7.85382	-2.07	-2.97	1.63	2.09
Pd	-5.2124	-3.01	-3.34	2.45	2.62
Ag	-3.20644	-0.52	-1.36	1.32	2.16
Cd	-1.07689	-1.84	--	--	--
Hf	-10.3627	-4.23	-5.22	-0.49	-0.25
Ta	-12.1566	-2.75	-2.40	0.32	0.20
W	-13.6431	-0.68	-1.83	0.33	0.71
Os	-11.25	-1.26	-1.53	1.00	0.81
Ir	-9.55728	-1.66	-2.71	1.71	2.06
Pt	-6.86285	-2.58	-3.66	2.47	3.01
Au	-3.87602	-1.18	-2.22	1.89	2.24

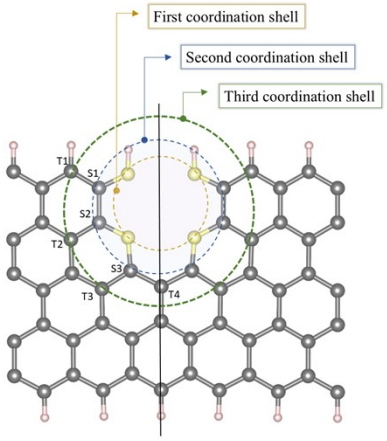

Figure S2. *Illustration of doping sites in the EN_4G B- and P- dopants at the 1st to 3rd coordination shells relative to the predefined N_4 sites*

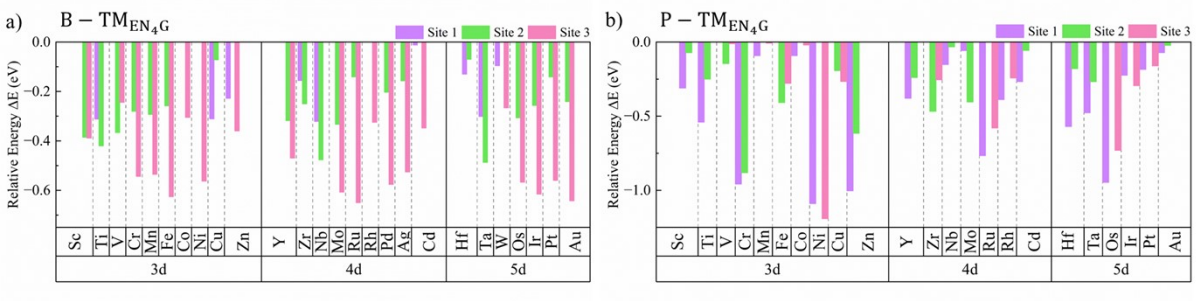

Figure S3. *Energy relative to their sites of (a) B- (b) P- doped EN_4G*

Table S2. *Bond lengths between TM atoms and the neighboring N atoms (*l_{TM-N_1}, l_{TM-N_2}, l_{TM-N_3}, l_{TM-N_4}, *Å) of optimized* $B-TM_{EN_4G}$ *structures and bond length (*$l_{B\text{-}N}$*) between B and N and distance (*D_B*) of B atoms relative to* EN_4G *plane.*

TM in N_4-C	Bond length (l) between TM and N in $B-TM_{EN_4G}$ (Å)						(Å)		Optimized Atomic Structures
	l_{TM-N_1}	l_{TM-N_2}	l_{TM-N_3}	l_{TM-N_4}	l_{avg}	D_m	$l_{B\text{-}N}$	D_B	
Sc	2.036	2.019	2.174	2.066	2.07	0.12	1.443	0.015	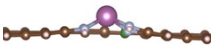
Ti	1.949	1.955	2.090	1.964	1.99	0.08	1.443	0.007	
V	1.906	1.897	2.056	1.959	1.95	0.09	1.443	0.012	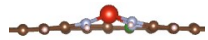
Cr	1.890	1.878	1.994	1.916	1.92	0.02	1.44	0.005	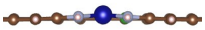
Mn	1.865	1.864	1.959	1.886	1.89	0.01	1.438	0.005	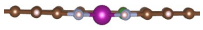
Fe	1.824	1.823	1.935	1.861	1.86	0.05	1.436	0.005	
Co	1.798	1.796	1.908	1.835	1.83	0.01	1.436	0.005	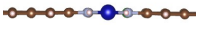
Ni	1.814	1.807	1.886	1.817	1.83	0.01	1.435	0.004	
Cu	1.853	1.837	1.917	1.839	1.86	0.01	1.428	0.002	
Zn	1.977	1.874	2.103	1.916	1.97	0.03	1.441	0.008	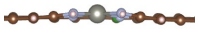
Y	2.204	2.184	2.343	2.212	2.23	0.12	1.445	0.008	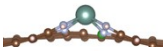
Zr	2.037	2.079	2.253	2.041	2.10	0.11	1.438	0.01	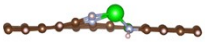
Nb	2.002	1.993	2.135	2.048	2.04	0.10	1.449	0.011	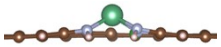
Mo	2.041	1.981	2.123	2.017	2.04	0.14	1.458	0.050.	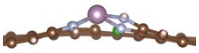
Ru	1.965	1.922	2.052	1.951	1.97	0.14	1.451	0.026	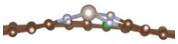
Rh	1.914	1.902	1.975	1.923	1.93	0.02	1.441	0.005	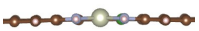
Pd	1.929	1.926	1.983	1.918	1.94	0.01	1.433	0.005	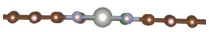
Ag	1.955	1.948	2.011	1.943	1.96	0.01	1.425	0.003	
Cd	2.183	2.1095	2.373	2.189	2.21	0.18	1.448	0.062	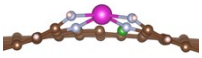
Hf	2.063	2.055	2.156	2.087	2.090	0.13	1.452	0.038	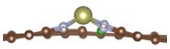
Ta	1.962	2.006	2.185	1.978	2.03	0.09	1.439	0.008	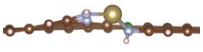
W	1.975	1.963	2.062	1.993	1.99	0.11	1.456	0.020	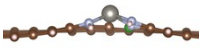
Os	1.925	1.88	2.000	1.946	1.94	0.08	1.449	0.02	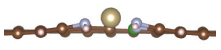
Ir	1.920	1.909	1.968	1.926	1.93	0.01	1.448	0.006	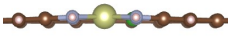
Pt	1.932	1.931	1.977	1.926	1.94	0.01	1.438	0.005	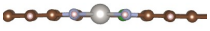
Au	1.947	1.955	1.998	1.945	1.96	0.02	1.429	0.006	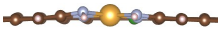

Table S3. Bond lengths between TM atoms and the neighboring N atoms (l_{TM-N_1}, l_{TM-N_2}, l_{TM-N_3}, l_{TM-N_4}, Å) of optimized $P-TM_{EN_4G}$ structures and bond length ($l_{P\text{-}N}$) between P and N and distance (D_P) of P atoms relative to EN_4G plane.

TM in N_4-C	Bond length (l) between TM and N in $P-TM_{EN_4G}$ (Å)								Optimized Atomic Structures
	l_{TM-N_1}	l_{TM-N_2}	l_{TM-N_3}	l_{TM-N_4}	l_{avg}	D_m	$L_{P\text{-}N}$	D_P	
Sc	2.03	2.05	2.20	2.15	2.11	0.11	1.69	0.09	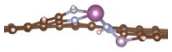
Ti	1.96	1.99	2.17	2.03	2.04	0.05	1.68	0.17	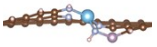
V	1.92	1.92	2.10	1.83	1.94	0.03	1.78	0.09	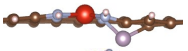
Cr	2.03	1.92	1.97	1.97	1.98	0.08	1.58	0.10	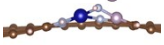
Mn	1.91	1.89	1.95	1.97	1.93	0.05	1.69	0.14	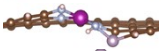
Fe	1.86	1.84	1.91	1.87	1.87	0.02	1.72	0.16	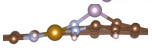
Co	1.88	1.82	1.86	1.87	1.86	0.06	1.63	0.05	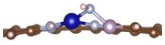
Ni	1.82	1.80	1.91	1.80	1.83	0.02	1.68	0.11	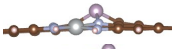
Cu	1.90	1.87	1.98	1.87	1.90	0.07	1.70	0.15	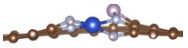
Zn	2.09	1.91	2.02	2.02	2.01	0.093	1.579	0.15	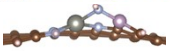
Y	2.17	2.19	2.35	2.29	2.25	0.149	1.688	0.11	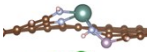
Zr	2.08	2.08	2.29	2.05	2.12	0.08	1.736	0.14	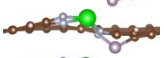
Nb	1.98	2.03	2.21	2.02	2.06	0.064	1.715	0.15	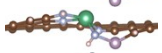
Mo	2.06	2.04	2.18	1.82	2.02	0.044	2.519	0.10	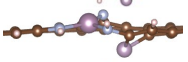
Ru	2.07	1.95	2.02	2.02	2.01	0.052	1.645	0.06	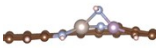
Rh	2.09	1.96	1.99	1.98	2.01	0.072	1.616	0.07	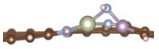
Cd	2.25	2.12	2.25	2.26	2.22	0.175	1.582	0.22	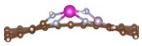
Hf	2.03	2.09	2.26	2.09	2.12	0.036	1.724	0.22	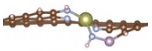
Ta	1.96	2.04	2.21	2.00	2.05	0.026	1.751	0.20	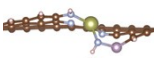
Os	1.95	1.93	2.01	1.92	1.95	0.098	1.695	0.09	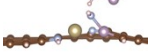
Ir	2.03	1.97	1.97	1.99	1.99	0.097	1.667	0.18	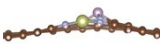
Pt	2.03	1.99	2.01	2.03	2.02	0.074	1.759	0.01	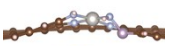
Au	2.03	2.05	2.20	2.15	2.11	0.1158	1.69	0.10	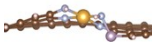

Table S4. Computed Gibbs free energies of ΔG_{O*}, ΔG_{OH*}, and ΔG_{OOH*} of all pristine-TM_{EN_4Gs}, $B-TM_{EN_4Gs}$ and $P-TM_{EN_4Gs}$ structures. The ΔG_{OOH*} values calculated according to the scaling relationship between ΔG_{OOH*} and ΔG_{OH*} are highlighted in blue.

TM in N_4-C	ΔG_{O*}			ΔG_{OH*}			ΔG_{OOH*}		
	pristine	B	P	pristine	B	P	pristine	B	P
Sc	1.51	1.75	0.70	-0.99	-0.65	0.70	2.17	2.66	2.39
Ti	-1.16	-0.66	-1.17	-1.75	-1.63	-1.17	1.71	1.89	2.05
V	-1.28	-1.13	-1.29	-1.36	-1.33	-1.29	2.05	2.14	2.31
Cr	-0.38	-0.46	-0.09	-0.15	-0.47	-0.09	3.10	2.86	3.28
Mn	0.67	0.75	0.87	0.57	0.60	0.87	3.82	3.81	3.79
Fe	1.43	1.62	1.63	0.67	0.68	0.81	3.84	3.87	3.98
Co	2.50	2.43	2.63	1.28	1.37	1.26	4.47	4.41	4.27
Ni	4.14	4.02	4.00	2.10	2.06	1.99	5.08	5.04	4.87
Cu	4.40	4.64	-0.47	2.24	2.35	2.13	5.04	5.33	5.20
Zn	3.86	3.92	1.63	1.47	1.53	0.81	4.44	4.79	3.98
Y	1.67	2.19	1.22	-0.89	-0.49	-0.96	2.46	2.92	2.57
Zr	-0.73	-0.85	-1.01	-2.33	-2.11	-2.09	1.20	1.35	1.64
Nb	-2.22	-2.57	-2.47	2.12	-2.11	-1.90	1.36	1.42	1.79
Mo	-2.22	-1.99	-1.72	-1.10	-1.47	-0.38	2.22	1.98	3.04
Ru	0.35	0.08	0.37	-0.02	-0.08	1.06	3.21	3.20	3.61
Rh	2.32	1.93	1.33	1.14	0.91	2.81	4.06	4.06	4.34
Pd	4.36	4.24	-	2.46	2.25	-	5.05	5.24	-
Ag	4.54	4.72	-	2.29	2.51	-	4.89	5.47	-
Cd	3.55	3.87	1.22	1.01	1.50	3.65	5.61	4.61	4.47
Hf	-1.36	-0.95	-1.29	-2.51	-2.41	-2.27	0.70	1.15	1.49
Ta	-2.84	-2.68	-2.49	-2.34	-2.27	-1.96	1.20	1.28	1.74
W	-2.98	-2.63	-	-2.20	-1.92	-	1.32	1.58	-
Os	-0.43	-0.54	0.55	-0.11	-0.57	0.45	2.36	2.77	3.72
Ir	1.92	1.75	1.96	0.83	0.59	1.08	4.16	3.80	4.23
Pt	4.06	3.88	3.48	2.42	2.32	2.59	5.35	5.24	5.47
Au	4.66	5.08	4.87	2.43	2.81	2.58	5.11	5.73	5.47

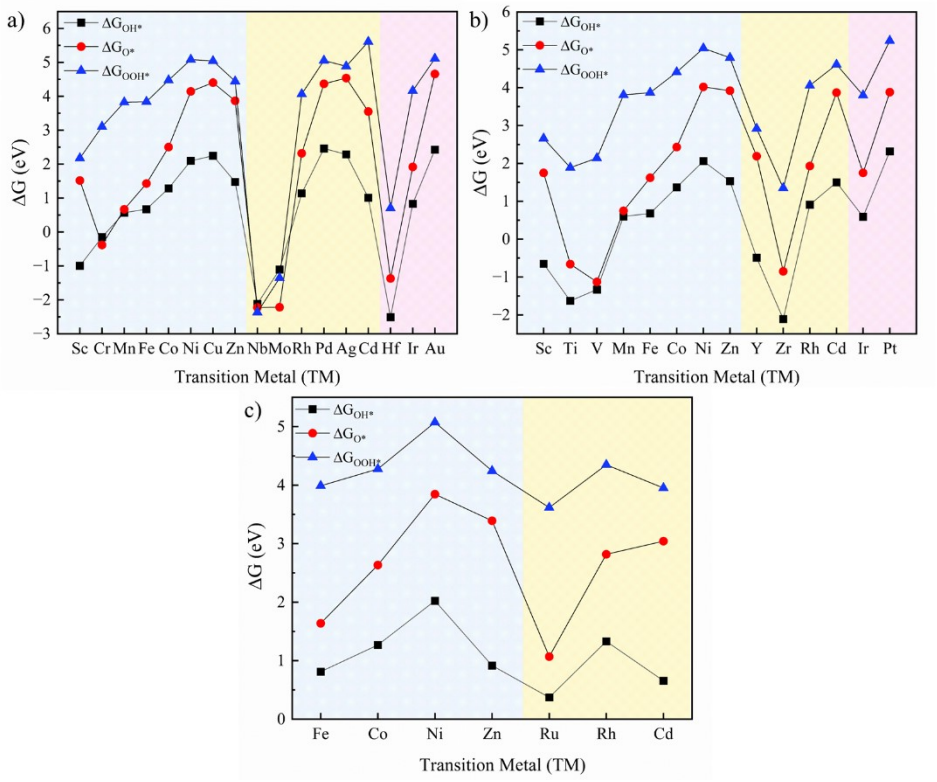

Figure S4. The ΔG_{O*}, ΔG_{OH*} and ΔG_{OOH*} values on different TM atoms in a) pristine-TM_{EN_4Gs},b) $B-TM_{EN_4Gs}$ and c) $P-TM_{EN_4Gs}$ systems

Table S5. Computed overpotential for OER(η_{OER}) and ORR(η_{ORR}) of all pristine-TM_{EN_4Gs}, $B-TM_{EN_4Gs}$ and $P-TM_{EN_4Gs}$ structures.

TM	η_{OER}			η_{ORR}		
	pristine	B	P	pristine	B	P
Sc	1.51	1.17	--	2.22	1.88	--
Ti	--	1.80	--	--	2.86	--
V	--	2.04	--	--	2.55	--
Cr	2.26	--	--	1.46	--	--
Mn	1.92	1.83	--	1.13	1.07	--
Fe	1.18	2.25	1.11	0.55	0.54	0.41
Co	0.74	0.75	0.41	0.78	0.72	0.58
Ni	0.87	0.82	0.77	1.39	1.34	1.18
Cu	1.01	--	4.45	1.35	--	3.84
Zn	1.16	1.15	1.11	0.75	1.10	0.41
Y	--	1.44	--	--	1.71	--

Zr	--	2.34	--	--	3.33	--
Nb	2.35	--	--	3.34	--	--
Mo	5.04	--	--	2.34	--	--
Ru	--	--	1.31	--	--	0.85
Rh	0.51	0.90	0.30	0.37	0.37	0.65
Pd	1.23	--	--	1.36	--	--
Ag	1.05	--	--	1.19	--	--
Cd	0.82	1.15	1.20	1.92	0.92	0.78
Hf	2.98	--	--	3.74	--	--
Ta	--	--	--	--	--	--
W	--	--	--	--	--	--
Os	--	--	--	--	--	--
Ir	1.01	--	--	0.47	--	--
Pt	--	1.08	--	--	1.55	--
Au	1.19	--	--	1.42	--	--

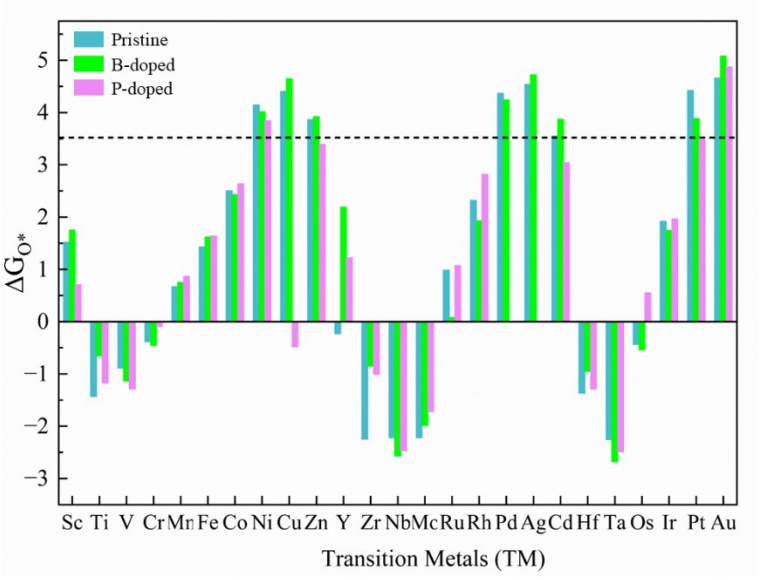

Figure S5. Path selectivity for H_2O and H_2O_2 formation ΔGO* values on different TM atoms in a) pristine-TM_{EN_4Gs},b) $B-TM_{EN_4Gs}$ and c) $P-TM_{EN_4Gs}$ systems

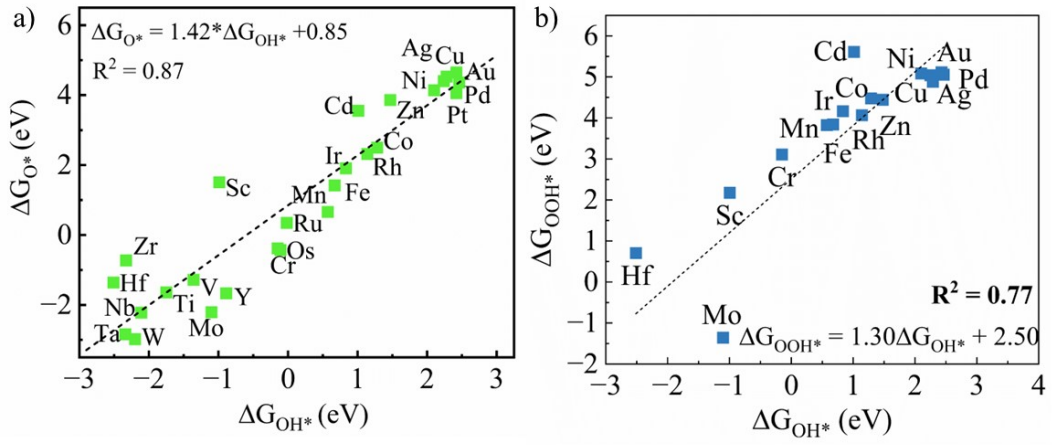

Figure S6. *Scaling Relationships of* a) ΔG_{O*} *vs.* ΔG_{OH*} b) ΔG_{OOH*} *vs.* ΔG_{OH*} in pristine-$TM_{EN_4}Gs$

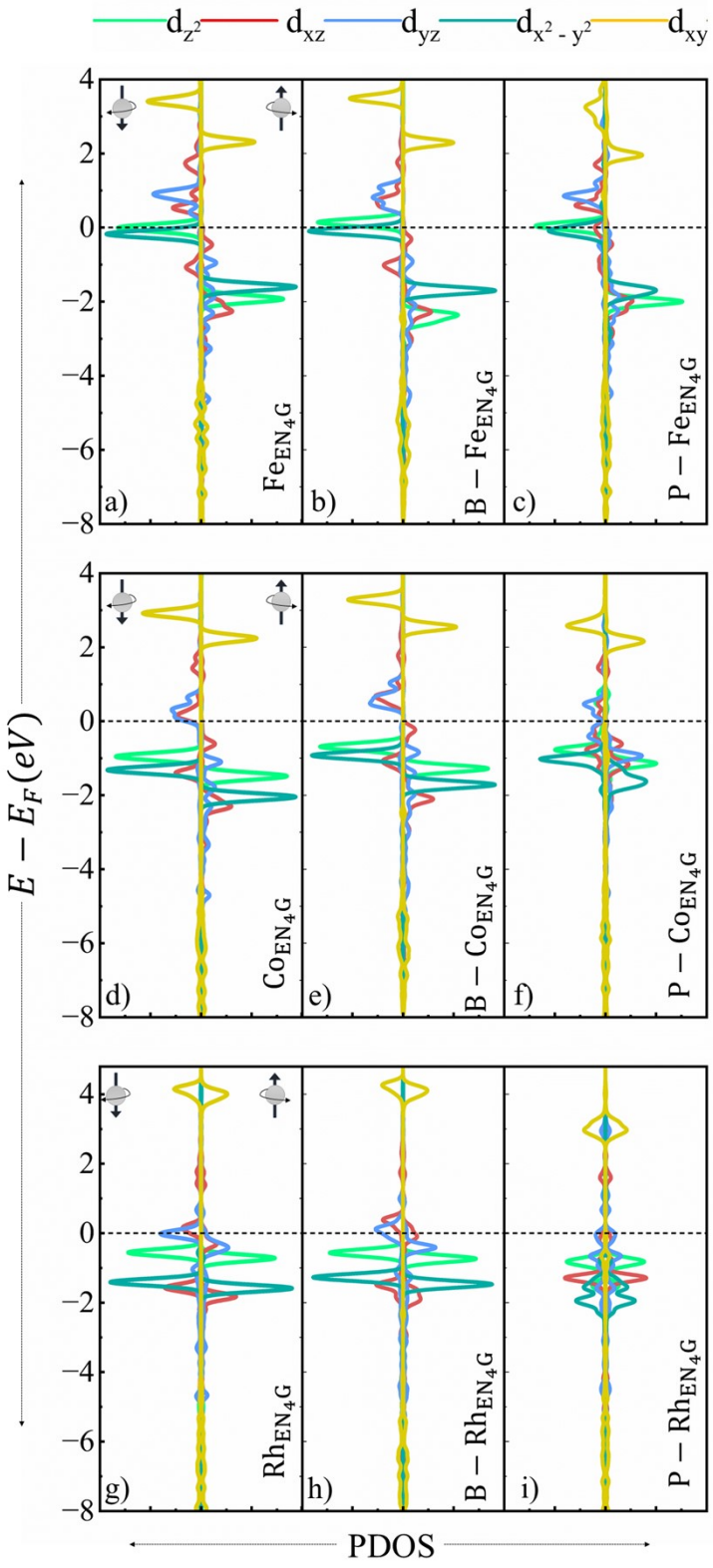

Figure S7. *PDOS of metal d-orbitals in pristine, B and P doped (a-c) Fe, (d-f) Co, and (g-i) Rh systems. The Fermi level is aligned to zero and indicated by a dashed line. Upward and downward arrows correspond to spin-up and spin-down channels, respectively.*

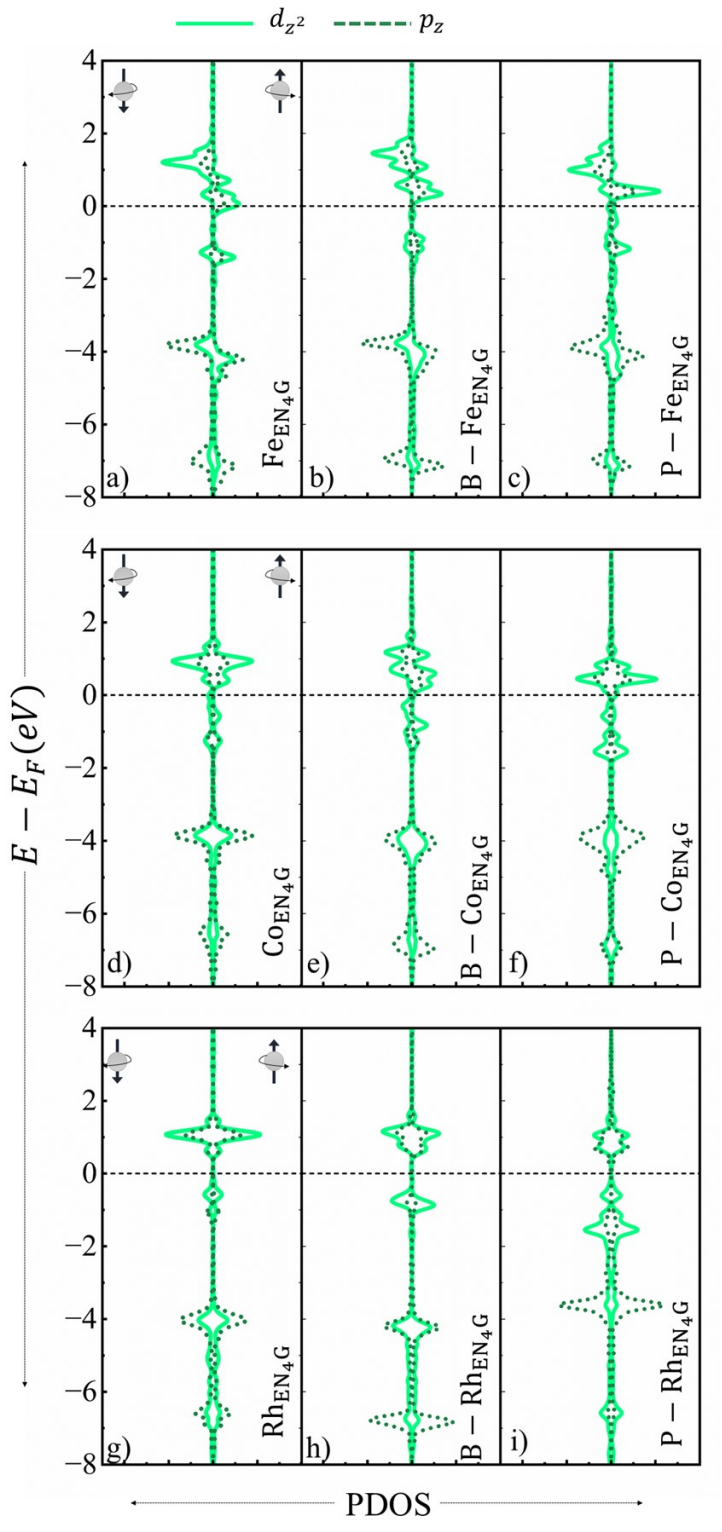

Figure S8. *PDOS of metal* $d_{z^2} - O_{p_z}$ *-orbitals for OH adsorbed on pristine, B and P doped (a-c) Fe, (d-f) Co, and (g-i) Rh systems. The Fermi level is aligned to zero and indicated by a dashed line. Upward and downward arrows correspond to spin-up and spin-down channels, respectively.*

Figure S9. *PDOS of metal $d_{xz,}\, d_{yz}$ -$O_{2p_{x,y}}$ -orbitals for OH adsorbed on pristine, B and P doped (a-c) Fe, (d-f) Co, and (g-i) Rh systems. The Fermi level is aligned to zero and indicated by a dashed line. Upward and downward arrows correspond to spin-up and spin-down channels, respectively.*

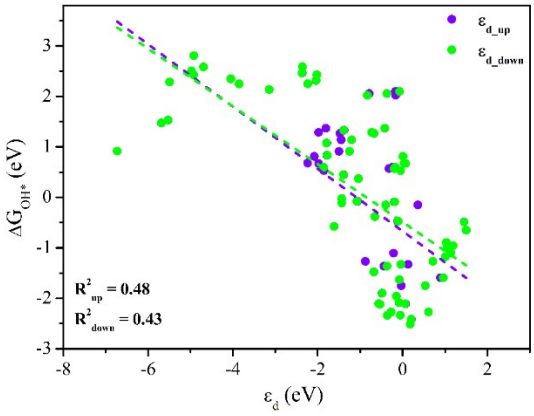

Figure S10. *Linear scaling relation between ΔG_{OH*} and ε_d for pristine, B-, and P-TM_{EN_4G}.*

Table S6. *Summary of the input features for ML model training*

	Features	Abbreviation
Atomic features	N_{TM}	Atomic number of the transition metal atom (TM)
	M_{TM}	Atomic mass of the TM
	R_{TM}	Atomic radius of the TM
	R_d	Zunger radius of the atomic d-orbital of the TM atom
	R_{cov}	Covalent radius of the TM atom
	N_d	Number of *d*-electrons of the TM atom
	n_e	Number of valence electrons of the TM atom
	E_I	First ionization energy of the TM atom
	E_A	Electron affinity of the TM atom
	$H_{f,ox}$	Oxide formation enthalpy of the TM atom
	EN_{TM}	Electronegativity of the TM atom
Electronic features	ε_{d_up}	*d*-band center of the upper DOS states of TM
	ε_{d_down}	*d*-band center of the lower DOS states of TM
	q_{TM}	Charge lost by the TM (Bader)
	d_{occup_up}	Occupancy of *d*-orbital states (up) of TM
	d_{occup_down}	Occupancy of *d*-orbital states (down) of TM
	q_{N1}	Charge on N1 atom
	q_{N2}	Charge on N2 atom
	q_{N3}	Charge on N3 atom
	q_{N4}	Charge on N4 atom
	d_{z^2}	d_{z^2} orbital occupancy
	d_{xz}	d_{xz} orbital occupancy
	d_{yz}	d_{yz} orbital occupancy
	$d_{x^2-y^2}$	$d_{x^2-y^2}$ orbital occupancy
	d_{xy}	d_{xy} orbital occupancy
Environmental features	$\bar{EN}_{TM\text{-}N}$	Average electronegativity of the surrounding nitrogen atoms and the TM
	$\bar{L}_{TM\text{-}N}$	Average bond lengths between the surrounding nitrogen atoms and the TM

Table S7*. Dataset of DFT-calculated parameters for pristine and B/P-doped TM_{EN_4Gs} used for ML model training.*

TM in EN_4-C	ε_{d_up}	ε_{d_down}	q_{TM}	d_{occup_up}	d_{occup_down}	q_{N1}	q_{N2}	q_{N3}	q_{N4}	d_{z^2}	d_{xz}	d_{yz}	$d_{x^2-y^2}$	d_{xy}
Sc	1.044	1.044	1.676	0.645	0.645	-1.303	-1.290	-1.335	-1.278	0.241	0.340	0.285	0.078	0.540
Ti	-0.031	0.537	1.499	1.61	0.734	-1.178	-1.256	-1.342	-1.275	0.845	0.431	0.332	0.134	0.325
V	-0.440	-0.368	1.425	1.6	1.61	-1.222	-1.279	-1.211	-1.281	0.795	0.456	0.352	1.174	0.625
Cr	0.358	-0.399	1.207	1.569	2.151	-1.309	-1.310	-1.248	-1.248	0.953	0.803	1.004	1.028	0.707
Mn	-0.321	-0.202	0.082	2.711	2.557	-1.125	-1.287	-1.155	-1.250	1.523	0.759	0.911	1.616	0.740
Fe	-1.980	0.072	1.124	4.16	2.16	-1.240	-1.292	-1.156	-1.253	1.367	1.235	1.147	1.794	0.816
Co	-1.982	-0.727	0.898	4.05	2.87	-1.078	-1.237	-1.207	-1.205	1.801	1.924	1.232	1.899	0.815
Ni	-0.168	-0.071	0.862	1.206	1.168	-1.092	-1.237	-1.102	-1.212	1.231	1.266	1.265	1.885	0.681
Cu	-3.856	-3.856	0.977	4.55	4.55	-1.222	-1.271	-1.177	-1.233	1.947	1.973	1.981	1.982	1.310
Zn	-5.687	-5.686	1.129	4.83	4.83	-1.321	-1.304	-1.289	-1.305	1.971	1.989	1.993	1.989	1.987
Y	1.030	1.030	2.003	0.663	0.663	-1.313	-1.327	-1.410	-1.313	0.142	0.376	0.364	0.389	0.495
Zr	-0.054	-0.054	1.924	1.088	1.089	-1.331	-1.255	-1.273	-1.197	0.551	0.524	0.454	0.374	0.595
Nb	-0.532	-0.530	1.648	1.733	1.718	-1.216	-1.288	-1.308	-1.273	0.836	0.600	0.518	1.104	0.684
Mo	-0.213	1.132	1.367	1.594	2.6	-1.250	-1.227	-1.213	-1.253	1.277	0.756	0.685	1.022	0.741
Ru	-1.435	-1.435	0.914	3.175	3.174	-1.078	-1.215	-1.079	-1.202	1.733	1.122	1.090	1.902	0.844
Rh	-1.450	-1.200	0.757	3.89	3.45	-1.090	-1.160	-1.116	-1.159	1.796	1.468	1.612	1.925	0.907
Pd	-2.368	-2.369	0.761	4.048	4.048	-1.106	-1.203	-1.117	-1.165	1.875	1.840	1.927	1.957	1.053
Ag	-5.494	-5.494	0.912	3.858	3.858	-1.237	-1.189	-1.176	-1.159	1.934	1.977	1.982	1.892	1.386
Hf	0.179	0.180	1.787	0.968	0.97	-1.187	-1.275	-1.239	-1.279	0.601	0.457	0.402	0.175	0.628
Ta	-0.360	-0.363	1.678	1.46	1.453	-1.323	-1.211	-1.294	-1.226	0.832	0.695	0.488	0.576	0.669
Os	-1.435	-1.434	1.040	2.93	2.93	-1.093	-1.213	-1.072	-1.198	1.690	1.052	0.985	1.880	0.865
Ir	-1.782	-1.777	0.848	3.431	3.439	-1.236	-1.219	-1.063	-1.185	1.745	1.422	1.550	1.912	0.950
Pt	-2.021	-2.021	0.798	3.822	3.822	-1.120	-1.207	-1.082	-1.188	1.804	1.766	1.887	1.943	0.980
Au	-4.923	-4.923	0.987	3.711	3.711	-1.272	-1.177	-1.185	-1.180	1.876	1.956	1.966	1.966	1.202
B-Sc	1.500	1.499	1.672	0.638	0.638	-1.222	-1.527	-1.226	-1.212	0.218	0.342	0.291	0.066	0.539
B-Ti	-0.077	-0.077	1.594	1.105	1.107	-1.287	-1.463	-1.224	-1.234	0.706	0.536	0.419	0.129	0.676
B-V	0.130	-0.040	1.466	1.607	1.595	-1.333	-1.497	-1.208	-1.233	0.691	0.452	0.350	1.169	0.629
B-Cr	-0.118	-0.106	1.271	2.165	2.093	-1.203	-1.539	-1.133	-1.272	1.745	0.747	0.541	1.818	0.756
B-Mn	-0.243	-0.171	1.353	2.63	2.562	-1.209	-1.495	-1.222	-1.238	1.342	0.930	0.920	1.379	0.787
B-Fe	-2.240	0.040	1.176	4.21	1.82	-1.125	-1.408	-1.134	-1.251	1.039	1.323	1.171	1.920	0.862
B-Co	-1.810	-0.420	0.884	4.1	2.77	-1.178	-1.363	-1.118	-1.176	1.812	1.336	1.199	1.903	0.844
B-Ni	-0.789	-0.369	0.889	1.287	1.008	-1.198	-1.361	-1.223	-1.161	1.203	1.264	1.055	1.214	1.323
B-Cu	-4.050	-4.050	0.954	4.31	4.47	-1.163	-1.375	-1.189	-1.173	1.950	1.977	1.981	1.983	1.368

B-Zn	-5.526	-5.531	1.118	4.833	4.834	-1.251	-1.497	-1.206	-1.213	1.971	1.990	1.993	1.990	1.980
B-Y	1.451	1.451	2.006	0.653	0.653	-1.322	-1.562	-1.294	-1.295	0.237	0.373	0.345	0.084	0.494
B-Zr	0.072	0.061	2.062	1.064	1.079	-1.298	-1.511	-1.308	-1.250	0.487	0.535	0.495	0.333	0.595
B-Nb	-0.565	-0.563	1.722	1.652	1.642	-1.233	-1.531	-1.291	-1.232	0.896	0.630	0.544	0.530	0.709
B-Mo	-0.676	-0.681	1.412	2.039	2.05	-1.205	-1.438	-1.285	-1.218	1.259	0.697	0.547	1.545	0.741
B-Ru	-1.060	-1.078	0.960	3.178	3.179	-1.126	-1.371	-1.044	-1.195	1.734	1.066	1.097	1.905	0.852
B-Rh	-1.500	-1.250	0.833	3.87	3.38	-1.190	-1.389	-1.158	-1.184	1.808	1.438	1.521	1.930	0.935
B-Pd	-2.238	-2.234	0.757	4.087	4.085	-1.205	-1.373	-1.177	-1.178	1.877	1.803	1.921	1.959	1.067
B-Ag	-4.979	-4.979	0.915	3.919	3.919	-1.186	-1.378	-1.219	-1.166	1.933	1.978	1.980	1.981	1.379
B-Hf	0.207	0.206	1.805	0.944	0.953	-1.232	-1.487	-1.260	-1.222	0.492	0.480	0.422	0.121	0.640
B-Ta	-0.270	-0.269	1.746	1.391	1.389	-1.311	-1.451	-1.212	-1.225	0.768	0.764	0.522	0.467	0.674
B-Os	-1.612	-1.614	1.096	2.912	2.908	-1.094	-1.385	-1.134	-1.152	1.700	0.962	0.968	1.884	0.879
B-Ir	-1.865	-1.862	0.930	3.42	3.418	-1.186	-1.384	-1.196	-1.193	1.755	1.354	1.551	1.915	0.969
B-Pt	-2.043	-2.038	0.808	3.79	3.787	-1.197	-1.386	-1.209	-1.160	1.803	1.718	1.874	1.941	0.992
B-Au	-4.922	-4.922	0.920	3.71	3.71	-1.159	-1.385	-1.119	-1.144	1.876	1.956	1.966	1.966	1.202
P-Sc	1.006	1.006	1.686	0.632	0.632	-1.604	-1.262	-1.310	-1.229	0.234	0.271	0.304	0.170	0.460
P-Ti	0.893	0.959	1.485	1.108	1.077	-1.588	-1.163	-1.250	-1.242	0.439	0.659	0.414	0.421	0.519
P-V	-0.879	0.714	1.455	2.281	0.87	-1.263	-1.479	-1.319	-1.262	0.921	0.911	0.502	0.484	0.697
P-Cr	-0.195	-0.188	1.253	1.955	2.097	-1.719	-1.180	-1.244	-1.236	0.273	0.937	0.784	1.144	0.671
P-Mn	-1.857	-0.045	1.331	4.14	1.013	-1.502	-1.244	-1.185	-1.168	1.103	1.132	1.163	1.076	0.874
P-Fe	-2.080	0.010	0.967	4.17	1.93	-1.151	-1.380	-1.167	-1.205	1.351	1.281	1.220	1.632	0.858
P-Co	-1.480	-0.670	0.860	3.93	3.11	-1.416	-1.144	-1.116	-1.198	1.591	1.532	1.412	1.866	0.838
P-Ni	-0.163	-0.832	0.844	0.984	1.335	-1.079	-1.393	-1.133	-1.230	1.217	1.265	1.032	1.218	1.323
P-Cu	-3.143	-3.144	0.926	4.581	4.581	-1.164	-1.407	-1.128	-1.202	1.952	1.964	1.973	1.978	1.451
P-Zn	-6.729	-6.729	1.148	4.748	4.748	-1.727	-1.171	-1.250	-1.262	1.984	1.987	1.992	1.991	1.985
P-Y	1.193	1.193	2.013	0.659	0.659	-1.661	-1.274	-1.358	-1.268	0.284	0.275	0.357	0.212	0.421
P-Zr	-0.086	-0.084	2.011	1.103	1.09	-1.255	-1.484	-1.414	-1.172	0.446	0.478	0.465	0.414	0.601
P-Nb	-0.486	-0.478	3.745	1.545	1.532	-1.532	-1.270	-1.235	-1.172	0.623	0.905	0.539	0.697	0.628
P-Mo	-0.653	-0.653	1.497	2.035	2.034	-1.203	-1.013	-1.320	-1.092	1.068	1.040	0.800	0.857	0.770
P-Ru	-1.040	-1.041	0.842	3.247	3.263	-1.426	-1.104	-1.221	-1.215	1.512	1.409	1.254	1.757	0.925
P-Rh	-1.380	-1.390	0.638	3.76	3.75	-1.427	-1.120	-1.242	-1.204	1.747	1.656	1.570	1.861	1.007
P-Hf	0.613	0.610	1.836	0.955	0.957	-1.530	-1.258	-1.370	-1.282	0.448	0.521	0.420	0.423	0.491
P-Ta	-0.148	-0.147	1.763	1.4	1.398	-1.464	-1.231	-1.250	-1.241	0.603	0.857	0.534	0.639	0.595
P-Os	-1.390	-1.394	0.950	3.06	3.059	-1.494	-1.182	-1.120	-1.213	1.485	1.319	1.143	1.741	0.928
P-Ir	-1.791	-1.795	0.858	3.457	3.461	-1.147	-1.355	-1.218	-1.182	1.742	1.319	1.580	1.886	0.953
P-Pt	-2.360	-2.360	0.718	3.896	3.896	-1.392	-1.147	-1.156	-1.149	1.788	1.823	1.870	1.937	1.039
P-Au	-4.693	-4.694	0.892	3.818	3.818	-1.257	-1.154	-1.085	-1.093	1.934	1.916	1.918	1.972	1.332

Table S8. *Hyperparameters configured for the various ML models studied.*

Model	Hyperparameters
SVR	kernel='linear' gamma='scale' random_state=0
RFR	n_estimators=200 max_depth=None random_state=0 min_samples_split=2 min_samples_leaf=1
LASSO	alpha=0.1 random_state=0
GBR	n_estimators=200 learning_rate=0.1 max_depth=3 random_state=0
XGB	n_estimators=200 max_depth=6 random_state=0 learning_rate=0.3

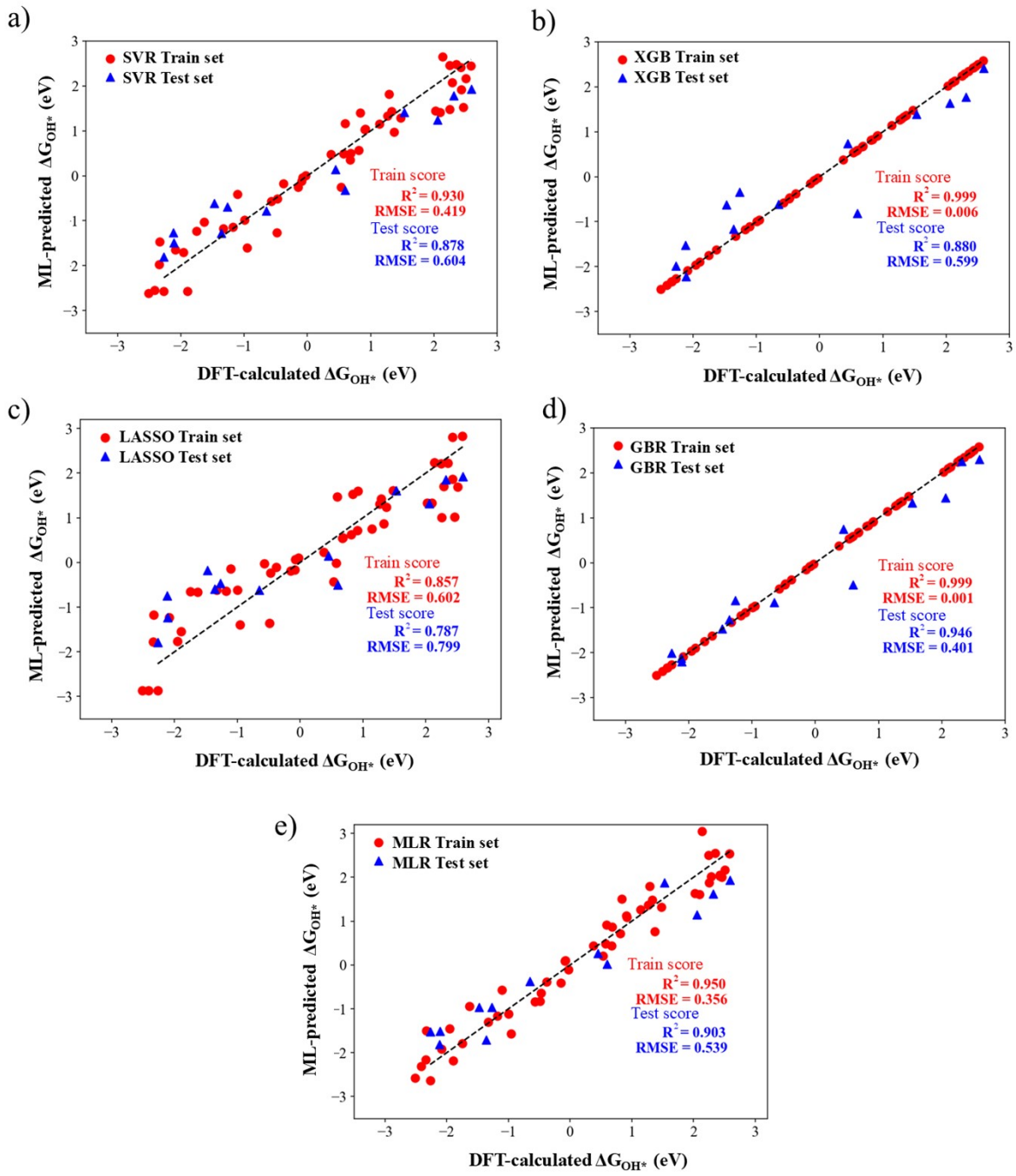

Figure S11. *ML-predicted Vs. DFT-calculated ΔG_{OH*} for a) SVR, b) XGB, c) LASSO, d) GBR, and e) MLR models.*

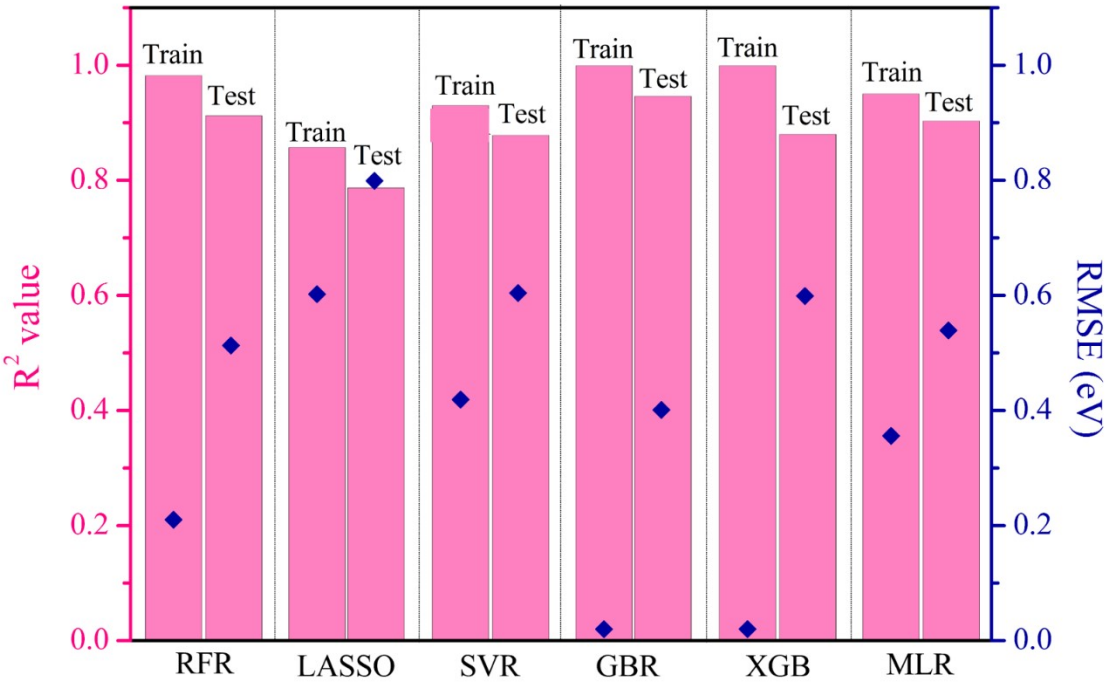

Figure S12. *Error diagram of the prediction performance of various ML models.*

References

1 Y. Zhang, J. Feng, C. Ma, X. Gu, L. Yu and L. Dong, *Appl Surf Sci*, 2025, 689, 162439.

2 Q. Liang, G. Brocks and A. Bieberle-Hütter, *Journal of Physics: Energy*, 2021, 3, 026001.

3 J. K. Nørskov, J. Rossmeisl, A. Logadottir, L. Lindqvist, J. R. Kitchin, T. Bligaard and H. Jónsson, *J Phys Chem B*, 2004, 108, 17886–17892.

4 Q. Ye, X. Yi, C. Wang, T. Zhang, Y. Liu, S. Lin and H. J. Fan, *Adv Funct Mater*, 2024, 34, 2400107.

5 J. Greeley and J. K. Nørskov, *Electrochim Acta*, 2007, 52, 5829–5836.

6 M. M. C. B. Neto, L. G. Verga, J. L. F. Da Silva and B. R. L. Galvão, *Physical Chemistry Chemical Physics*, 2023, 25, 4939–4949.

7 W. Li, G. Feng, S. Wang, X. Zhong, Z. Yao, S. Deng and J. Wang, *J Mater Chem A Mater*, 2023, 11, 15426–15436.

8 Y. Ying, K. Fan, X. Luo, J. Qiao and H. Huang, *J Mater Chem A Mater*, 2021, 9, 16860–16867.